Available online at www.sciencedirect.com
SCIENCE DIRECT®
Journal of Non-Crystalline Solids 351 (2005) 2388–2393
JOURNAL OF NON-CRYSTALLINE SOLIDS
www.elsevier.com/locate/jnoncrysol

Investigations on bismuth and aluminum co-doped germanium oxide glasses for ultra-broadband optical amplification

Mingying Peng [a,b,*], Chen Wang [a,b], Danping Chen [a], Jianrong Qiu [a,*], Xiongwei Jiang [a], Congshan Zhu [a]

[a] Shanghai Institute of Optics and Fine Mechanics, Chinese Academy of Science, Shanghai 201800, China
[b] Graduate School of the Chinese Academy of Sciences, Beijing 100039, China

Received 5 December 2004; received in revised form 22 June 2005

Abstract

The broadband luminescence covering 1.2–1.6 μm was observed from bismuth and aluminum co-doped germanium oxide glasses pumped by 808 nm laser at room temperature. The spectroscopic properties of GeO_2:Bi,Al glasses strongly depend on the glass compositions and the pumping sources. To a certain extent, the Al^{3+} ions play as dispersing reagent for the infrared-emission centers in the GeO_2:Bi,Al glasses. The broad infrared luminescence with a full width at half maximum larger than 200 nm and a lifetime longer than 200 μs possesses these glasses with the potential applications in broadly tunable laser sources and ultra-broadband fiber amplifiers in optical communication field.

PACS: 42.70.Km; 78.60.−b; 78.20.Ci; 42.60.Da

1. Introduction

The demand for the information transportation system with much higher transmission capacity and much faster bit rates results in the extraordinarily increasing utilization of the wavelength division multiplexing (WDM) system in the telecommunication field [1]. To achieve the more efficient WDM transmission network, one of attractive approaches is to increase the transmission-channel number through broadening the gain bandwidth of the laser sources and the fiber amplifiers. Therefore, exploration of new broadband luminescent materials especially covering the 1.2–1.6 μm region and possessing much larger full width at half maximum (FWHM) becomes a key step to further develop the broadband fiber amplifiers and the broadly tunable laser sources. In the past years, more studies have been performed on the rare earth ion, e.g., Er^{3+}, Tm^{3+} or Pr^{3+}, doped materials [2,3]. However, the work bandwidths of such materials hardly surpass 100 nm since the emissions in near infrared region are mainly initiated from the forbidden f–f transitions between the inner-shell 4f orbits of the rare earth ions. On the contrary, the broad emissions with FWHM larger than 100 nm can be easily achieved with transition-metal-ion-doped materials, because the emissions originate from the d–d transitions of transition-metal ions [4–6]. For example, broadband emission in 1.2–1.6 μm was observed with FWHM wider than 200 nm from Cr^{4+}- or Ni^{2+}-doped glasses [5,6]. Recently, Fujimoto and Nakatsuka reported a novel infrared luminescence from bismuth-doped silicate glass and realized its optical amplification

* Corresponding authors. Address: Shanghai Institute of Optics and Fine Mechanics, Chinese Academy of Science, Shanghai 201800, China (M. Peng).
E-mail addresses: mypeng@mail.siom.ac.cn (M. Peng), jrq@photon.jst.go.jp (J. Qiu).

0022-3093/$ - see front matter © 2005 Elsevier B.V. All rights reserved.
doi:10.1016/j.jnoncrysol.2005.06.033

at 1.3 μm with 0.8 μm excitation [7,8]. Subsequently, our group also observed the 1.3 μm emission with FWHM more than 300 nm in aluminum and bismuth co-doped germanium oxide glasses pumped by the 808 nm laser diode [9]. All the previous works have clearly demonstrated that co-doping of aluminum into bismuth-doped glasses is indispensable for the occurrence of the broadband infrared luminescence [7,9]. However, it is still unknown up to now what role the aluminum ion plays in the generation of infrared luminescence. In addition, no systematic investigations have been carried out on the effect of the principle glass composition on luminescent properties of GeO_2:Bi,Al glasses.

In this work, we firstly investigate the effects of the bismuth or aluminum concentrations and the pumping sources on the luminescent properties of GeO_2:Bi,Al glasses, and then study the possible role of aluminum in infrared luminescence of GeO_2:Bi,Al glasses and finally discuss the luminescent mechanism.

2. Experimental

The compositions of the glass samples prepared in this study are $(100 - x - y)GeO_2 \cdot xBi_2O_3 \cdot yAl_2O_3$ where $x = 0$, 0.01, 0.05, 0.1, 0.5, 1.0, 1.5, 2.0 and $y = 0$, 1, 2, 3, 4, 5, 6, 8, respectively. Twenty grams batch for each sample was prepared from commercial powders of high-purity GeO_2 (99.999%), analytic reagent $Al(OH)_3$ and Bi_2O_3 by mixing homogenously in an agate mortar. Each batch was melted at 1540 °C in a high-pure alumina crucible for 20 min in air, and then quickly cast onto a stainless steel plate and finally annealed at 600 °C for 2 h. All the prepared and selected glass samples were transparent and bubble-free through the inspection by an optical microscope. The glass specimens were cut and polished into the appropriate shape and thickness for measurements.

All the samples were confirmed to be amorphous by X-ray diffraction (XRD) patterns recorded on a Bruker D4 X-ray diffractometer at 40 kV/20 mA with Cu Kα1 ($\lambda = 1.5405$ Å) as a radiation source. Absorption spectra were recorded with JASCO V-570 spectrophotometer from 400 to 1500 nm using the sample with a thickness of approximately 1 mm. Infrared emission spectra were measured using ZOLIX SBP300 spectrofluorometer with InGaAs as detector in 850–1800 nm. A 50 mW double frequency YAG: Nd laser with 532 nm wavelength, a 50 mW He–Ne laser with 632.8 nm wavelength and a 135 mW InGaAs semiconductor laser diode with 808 nm wavelength were chosen as the excitation sources. Lifetime measurements were carried out by exciting the sample with a modulated 808 nm laser diode with a maximum power of 2 W. The signal detected by an InGaAs photodetector in TRIAX550 was recorded using a Tektronix TDS3052 storage digital oscilloscope. X-band ESR spectra in the case of $v = 9.82$ GHz were obtained with a Bruker model ER200D-SRC spectrometer under microwave power of 20 MW. The polished glass sample hardness was measured using a HXD-1000 microhardness instrument under an applied load of 100 g. The refractive index was measured on the prism minimum deviation method. All the above measurements were taken at room temperature. Differential thermal analysis (DTA) curve was measured with a CRY-Z Differential Thermal Analyzer at a heating rate of 10 °C min^{-1} using aluminum oxide ceramic pans.

3. Results

3.1. Effect of bismuth concentration

Figs. 1 and 2 show the absorption and fluorescent spectra of $(97 - x)GeO_2 \cdot xBi_2O_3 \cdot 3Al_2O_3$ ($x = 0.01$, 0.05, 0.1, 0.5, 1.0, 1.5, 2.0) glasses, respectively. As can be seen from Fig. 1, there are four absorption peaks at about 500, 700, 800 and 1000 nm, respectively. With the bismuth concentration increasing, the peak of the 500 nm band shifts towards shorter wavelength from about 560 nm gradually to 500 nm while the peak of the 700 nm band shifts towards the reverse direction. And the latter two bands remain almost unshift. At the same time, as shown in Fig. 2, the strongest emission peak moves towards longer wavelength, viz. 1100 nm for $x = 0.01 \rightarrow 1254$ nm for $x = 0.05 \rightarrow 1260$ nm for $x = 0.1 \rightarrow 1284$ nm for $x = 0.5 \rightarrow 1300$ nm for $x = 1.0 \rightarrow 1305$ nm for $x = 1.5 \rightarrow 1310$ nm for $x = 2.0$. Furthermore, with increasing x value, the fluorescent intensity monotonically increases until $x = 0.5$, and then decreases, showing that the critical dopant concentration is about 0.5 mol%.

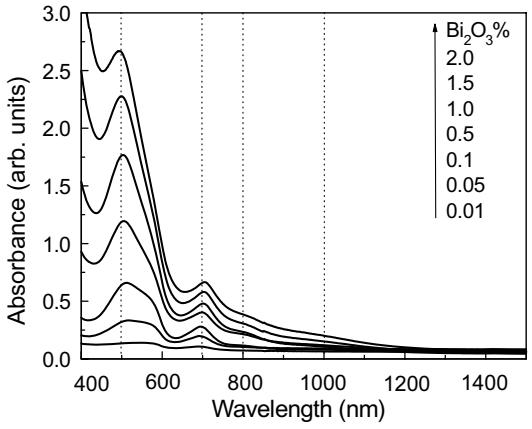

Fig. 1. Absorption spectra of $(97 - x)GeO_2 \cdot 3Al_2O_3 \cdot xBi_2O_3$ ($x = 0.01$, 0.05, 0.1, 0.5, 1.0, 1.5, 2.0) glasses.

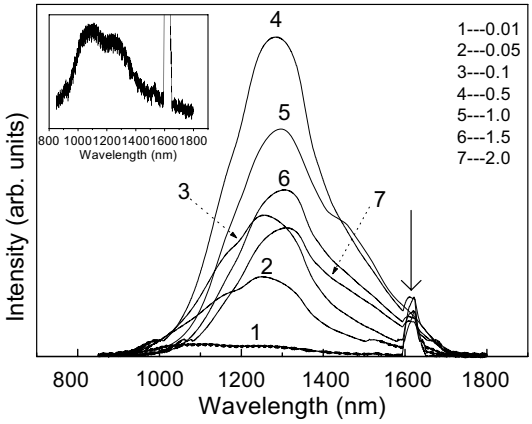

Fig. 2. Fluorescent spectra of $(97-x)GeO_2{\cdot}3Al_2O_3{\cdot}xBi_2O_3$ ($x=0.01$, 0.05, 0.1, 0.5, 1.0, 1.5, 2.0) glasses when pumped by 808 nm. The inset is the amplified spectrum of $96.99GeO_2{\cdot}\ 3Al_2O_3{\cdot}0.01Bi_2O_3$. The peaks indicated by arrow are due to the second-order diffraction of 808-nm laser.

3.2. Effect of aluminum concentration

Fig. 3 illustrates the fluorescent spectra of $(99-y)$-$GeO_2{\cdot}1.0Bi_2O_3{\cdot}yAl_2O_3$ ($y=1,3,5,8$) pumped by 808 nm laser. Fig. 4 shows the integrated fluorescent intensity and lifetime as function of Al_2O_3 concentration. As y value increasing, the fluorescent intensity continuously increases until $y=5.0$, and then decreases as shown in Figs. 3 and 4. Meanwhile, the emission peak shifts from 1320 nm ($y=1.0$), 1300 nm ($y=3.0$), 1300 nm ($y=5.0$) to 1286 nm ($y=8.0$). Obviously, the influence of Al_2O_3 addition on the fluorescent peak position seems slighter than that of the Bi_2O_3 addition.

3.3. Effect of pumping sources

Fig. 5 presents the normalized fluorescent spectra of $96GeO_2{\cdot}1.0Bi_2O_3{\cdot}3Al_2O_3$ glass in the case of different excitation schemes. With pumping-source variation from 532 nm to 632.8 nm and 808 nm, the strongest emission peak shifts towards longer wavelength, viz. 1247 nm (FWHM = 295 nm) → 1263 nm (FWHM = 281 nm) → 1300 nm (FWHM = 320 nm), and the shoulder peak at around 1170 nm vanishes gradually, indicating the fluorescence dependence on the pumping source. Similar result was also found in bismuth doped silicate glasses [7]. The fluorescence dependence on the excitation sources provides the possibility to optimize the pumping routes for the optical amplifications.

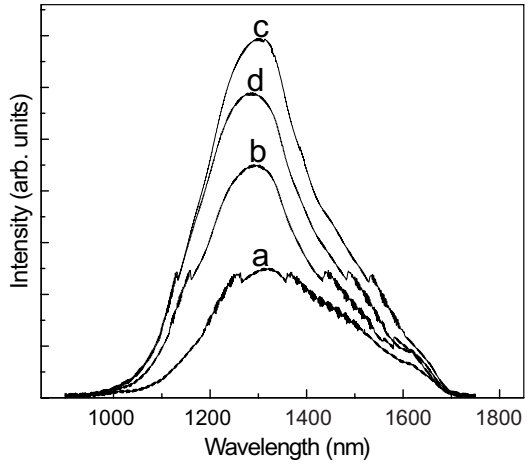

Fig. 3. Fluorescence spectra of $(99-x)GeO_2{\cdot}xAl_2O_3{\cdot}1Bi_2O_3$ ($x=1.0$, 3.0, 5.0, 8.0) glasses when pumped by 808 nm.

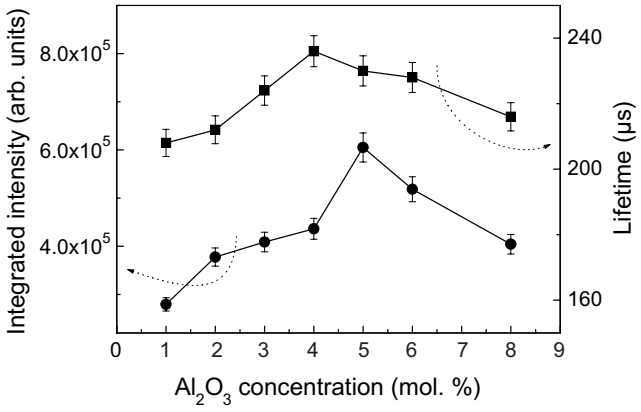

Fig. 4. The integrated fluorescent intensity (●) and lifetime (■) of $(99-x)GeO_2{\cdot}xAl_2O_3{\cdot}1Bi_2O_3$ ($x=1.0$, 2.0, 3.0, 4.0, 5.0, 6.0, 8.0). Lines are drawn as guides for the eye.

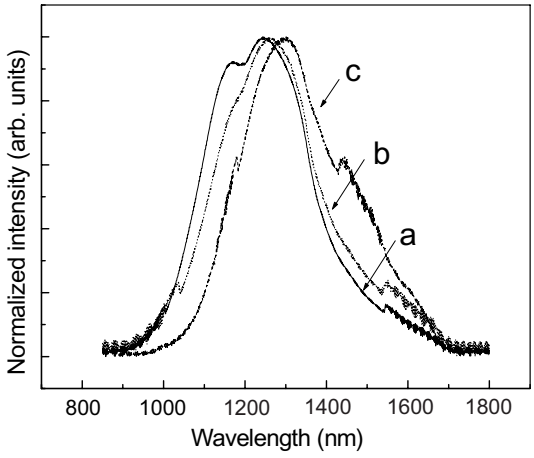

Fig. 5. Normalized fluorescence spectra of $96GeO_2{\cdot}3Al_2O_3{\cdot}1Bi_2O_3$ by different excitation sources: (a) 532 nm, (b) 632.8 nm and (c) 808 nm.

3.4. Thermal, mechanical and optical properties of $94.5GeO_2{\cdot}5Al_2O_3{\cdot}0.5Bi_2O_3$ glass

Based on the studies on Sections 3.1 and 3.2, the glass sample with optimized composition of $94.5GeO_2{\cdot}\ 5Al_2O_3{\cdot}0.5Bi_2O_3$ (GAB) was prepared. The DTA data of GAB glass show that the glass transition temperature T_g, the crystallization onset temperature T_x and the

maximum crystallization temperature T_c are 651, 757 and 779 °C, respectively. Glass thermal stability roughly characterized by the parameter $\Delta T = T_x - T_g$ can be considered to be better if $\Delta T > 100$ °C [10]. The GAB glass is stable against devitrification due to its larger ΔT value up to 106 °C.

Vicker's hardness of GAB glass was measured to be 274 kg mm^{-2}, a little bigger than 264 kg mm^{-2} for the $91GeO_2 \cdot 8Al_2O_3 \cdot 1Bi_2O_3$ glass. The hardness decrement partially reflects that the glass network becomes looser as Al_2O_3 concentration increases.

The absorption cross-section (σ_{ab}) at 808 nm for GAB glass was calculated to be 1.61×10^{-20} cm^2. The stimulated emission cross-section (σ_{em}) at 1280 nm was estimated to be 1.55×10^{-20} cm^2 by Füchtbauer–Landenburg equation: $\sigma_{em} = \frac{\lambda^4}{8\pi n^2 c \cdot \Delta\lambda} \cdot \frac{1}{\tau_{rad}} \cdot g(\lambda)$ where λ is wavelength, $g(\lambda)$ is the normalized spontaneous emission shape function, n is the host refractive index, c is light velocity, $\Delta\lambda$ is the FWHM of emission and τ_{rad} is the emission lifetime [11]. In this work, $\Delta\lambda = 322$ nm, $\tau_{rad} = 273$ μs and $n = 1.6166$, respectively for GAB glass.

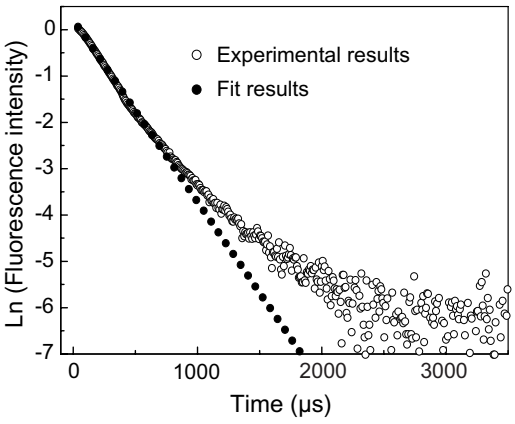

Fig. 6. Fluorescence decay curve of $96GeO_2 \cdot 3Al_2O_3 \cdot 1.0Bi_2O_3$ glass when pumped by 808 nm. It was measured by monitoring at emission of 1300 nm at room temperature. The correlation coefficient for the fit by the first-order exponential decay equation ($y = 1.24475e^{(-t/254.5)}$) is 0.99853.

4. Discussion

4.1. Absorption and emission spectra

As can be seen from the absorption and emission spectra of the series of $(97 - x)GeO_2 \cdot xBi_2O_3 \cdot 3Al_2O_3$ ($x = 0.01$, 0.05, 0.1, 0.5, 1.0, 1.5, 2.0) glasses (see Figs. 1 and 2), the strongest emission lies at ~1100 nm with a shoulder peak at about 1254 nm and the strongest absorption lies at about 560 nm with a shoulder peak at about 510 nm when $x = 0.01$. Along with increasing the x value to 0.05, the 1254 nm emission and the 510 nm absorption becomes the strongest whereas the 1100 nm emission and the 560 nm absorption becomes a shoulder. As x value further increases to 1.0, the ~1300 nm emission turns into the strongest with appearance of another new shoulder peak at 1450 nm except the 1100 nm shoulder, meanwhile the strongest absorption moves to ~500 nm. We propose that at least four emission centers, e.g., 1100, 1254, 1300 or 1450 nm emission centers, exist in these glasses, which might be the reason why the fluorescence decay curve of $96GeO_2 \cdot 1Bi_2O_3 \cdot 3Al_2O_3$ is not just a simple exponential decay (see Fig. 6). Previously, we considered the fluorescence decay to obey the first-order exponential equation [9]. But as we redraw the figure with the intensity in natural logarithm against decay time, the divergence between the fluorescence decay curve and the first-order exponential equation clearly protrudes in the latter stage even though the decay curve is consistent with the first-order exponential equation in the initial stage. At lower bismuth concentration, the 1100-nm emission center is preferred; while at higher bismuth concentration, the other centers can be favored to form, which results in the shape changes in both absorption and emission spectra.

4.2. The role of aluminum in the infrared luminescence

The coordination number of aluminum ion increases with increasing Al_2O_3 content in Al_2O_3–SiO_2 glass [12]. As a small amount of Al_2O_3 is built into the Al_2O_3–SiO_2 glass, Al^{3+} ions will be mainly in the four-fold coordination [12–17]. In view of the much more structural resemblance between glassy SiO_2 and GeO_2, the $[AlO_{4/2}]^-$ tetrahedrons will be more favorable in GeO_2-based glasses because the ion radius of Ge^{4+}($R^{4+}_{Ge}(CN = 4) = 0.39$ Å where CN is the coordination number) matches that of Al^{3+}($R^{3+}_{Al}(CN = 4) = 0.39$ Å) better than that of Si^{4+}($R^{4+}_{Si}(CN = 4) = 0.26$ Å) [18]. When the Al_2O_3 concentration is as lower as $y < 4.0$, the formed $[AlO_{4/2}]^-$ tetrahedrons coupled with $[GeO_4]$ tetrahedrons will surround the bismuth-related infrared-emission centers and enlarge the center-to-center spacing in the bonding association of Al–O–Bi, which is similar to the dispersing of the Nd^{3+} ions by Al^{3+} ions in Nd^{3+} and Al^{3+} co-doped silica glasses [12–15]. Consequently, the interaction between these emission centers will be weakened and the energy loss due to non-radiation transitions will be reduced. Therefore the fluorescent intensity and lifetime increases as indicated in Fig. 4. However, when the Al_2O_3 concentration becomes as higher as $5.0 < y < 8.0$, the five- or six-coordinated Al^{3+} ions, coexisting with four-coordinated ones, appear and increase [12,15]. The five- or six-coordinated Al^{3+} ions play as the glass network modifiers and could not efficiently disperse the infrared-emission centers. Thus, the interaction between the

infrared-emission centers becomes stronger, and the fluorescent intensity and lifetime decreases as shown in Fig. 4.

In the preparation process of GeO_2:Bi,Al glass, we observed that the glass molten becomes more easily poured out of the alumina crucibles with increasing the Al_2O_3 concentration, which might be attributed to the increasing non-bridging oxygen ions with increasing network modifiers of five- or six-coordinated Al^{3+} ions. When y is up to 10, no transparent glass could be obtained.

4.3. Where does the broad infrared luminescence come from?

In the past decades, luminescent properties of Bi^{3+} or Bi^{2+} doped crystals and glasses have been investigated [19–24]. The Bi^{3+} transitions between the ground state ($^1S_0$) and the excited states ($^3P_1$ and $^1P_1$ mixed by the spin–orbit coupling) are usually observed [19]. The absorption (or excitation) peaks of Bi^{3+} in both crystals and glasses appear in the ultraviolet region, while the emission peaks of Bi^{3+} occurs in the ultraviolet, green, or even red wavelength region corresponding to the variation of host materials [19–22]. But no infrared luminescence from Bi^{3+} and no fluorescent lifetime of Bi^{3+} longer than 5 μs in crystals or glasses have been reported up to now [19,22]. Contrary to Bi^{3+}-doped luminescent materials, Bi^{2+}-doped ones were paid little attentions. To the best of our knowledge, only the luminescent properties of Bi^{2+} in crystals were reported. The Bi^{2+} transition between the ground state of $^2P_{1/2}$ and the first excited state of $^2P_{3/2}$ is parity forbidden, but becomes allowed when $^2P_{1/2}$ and the excited states of $^2S_{1/2}$ and $^2P_{3/2}$ are mixed by the uneven crystal-field terms, whereas the transition between $^2P_{1/2}$ and $^2S_{1/2}$ is strongly allowed [13,14]. Therefore, three excitation peaks of Bi^{2+} in SrB_4O_7 corresponding to the transitions from $^2P_{1/2}$ to $^2P_{3/2}$ split into two by crystal fields and to $^2S_{1/2}$ were observed at 575, 470 and <312 nm, and one emission peak of $^2P_{3/2} \rightarrow {}^2P_{1/2}$ was at 586 nm [23]. And the fluorescent lifetime of SrB_4O_7:Bi^{2+} was 10.6 μs at 300 K [23].

Compared with the information on the Bi^{3+} or Bi^{2+} doped materials mentioned above, the absorption and emission peak-positions of GeO_2:Bi,Al glasses are greatly different from the Bi^{3+} or Bi^{2+} doped materials. Four absorption peaks of GeO_2:Bi,Al glasses cover the large wavelength region from visible to infrared, and their emission peaks lie in the infrared region. Furthermore the fluorescent lifetimes of GeO_2:Bi,Al glasses are more than 200 μs, which are one order or two order longer than those of the aforementioned Bi^{2+} or Bi^{3+} doped materials. Fujimoto et al. ascribed the absorption and the emission spectra of Bi and Al ions co-doping silicate glasses to the Bi^{5+} transitions between the ground state of $^1S_0$ and the excited states of $^3D_{3,\,2,\,1}$ and $^1D_2$ [7]. But as well known, Bi^{5+} ions are confirmed to exist in compounds containing alkali oxides with higher basicity, e.g., in $NaBiO_3$ or $KBiO_3$, which are absent in GeO_2:Bi,Al glasses [25,26]. Moreover, at higher temperature, Bi_2O_3 will readily dissociate into the black suboxide BiO or into bismuth metal [27]. ESR measurement is employed to detect the paramagnetic centers like Bi^{2+} ions. Unfortunately no signal could be detected, which is similar to Ref. [7].

Dong and Zhu studied the optical properties of the surface-modified Bi_2O_3 nanoparticles in the size range of 5–13 nm [28]. One exciton-absorption peak at 484 nm and the absorption band gap of ~ 376 nm (~ 3.3 eV) were reported for both orange and wine-red Bi_2O_3 nanoparticles, which was very close to the absorption peak of ~ 500 nm and the absorption edge of ~ 375 nm in GeO_2:Bi,Al glasses [9]. But no infrared luminescence was investigated in such Bi_2O_3 nanoparticles. As examined by the X-ray diffractometer, no obvious signals indicate the existence of Bi_2O_3 phase in the GeO_2:Bi,Al glasses. Therefore there are two possibilities. One is that the infrared luminescence is not from Bi_2O_3 nanoparticles. The other is that the infrared luminescence is from the Bi_2O_3 nanoparticles, but the amount of Bi_2O_3 is too small to be detected by the X-ray diffractometer. If the infrared luminescence comes from the Bi_2O_3 nanoparticles indeed, it should not be arising from the direct transitions from conduction band to valence band since the band gap energy of Bi_2O_3 is about 3.3 eV [28]. It might be from recombinations between the defect levels in the band gap or from the defect levels to the valence band. In order to identify what types of bismuth really contribute to the infrared luminescence, more investigations should be carried out even though the spectral features of the GeO_2:Bi,Al glasses are similar to those of the SiO_2: Al, Bi glasses.

4.4. Figure-of-merits of bandwidth and gain

As well known, the products of $\sigma_{em} \times \mathrm{FWHM}$ and $\sigma_{em} \times \tau$ are the important parameters to evaluate the figure-of-merit of bandwidth and gain of broadband amplifier, respectively [6,29]. The bigger the products, the better the bandwidth and gain properties of the amplifiers. The parameters of $\sigma_{em} \times \mathrm{FWHM}$ and $\sigma_{em} \times \tau$ for the GAB glass are about 499×10^{-20} cm^2 nm and 4.23×10^{-24} cm^2 s, respectively, which are bigger than that for Er^{3+}-doped silicate glass ($\sigma_{em} \times \mathrm{FWHM} = 22 \times 10^{-20}$ cm^2 nm) [29], that for Cr-doped foresterite ($\sigma_{em} \times \tau = 2.85 \times 10^{-24}$ cm^2 s) [11] and that for Ti-doped sapphire ($\sigma_{em} \times \tau = 1.4 \times 10^{-24}$ cm^2 s) [6]. Therefore, it can be suggested from the above comparison that the Bi- and Al-co-doped germanium oxide glass might be the promising host material for the super-broadband amplifiers.

5. Conclusions

The broad near infrared emission, which was greatly different from those Bi^{3+}- or Bi^{2+}-doped materials previously reported in the literatures, was observed in the spectral region of 1.2–1.6 μm from GeO_2:Bi,Al glasses at room temperature in the case of 808 nm excitation. The luminescent properties of GeO_2:Bi,Al glasses depend on the glass compositions. The Al^{3+} ions play as dispersing role for the infrared-emission centers in GeO_2:Bi,Al glasses. The broad infrared luminescence with FWHM more than 200 nm and lifetime longer than 200 μs covers the O (1260–1360 nm), E (1360–1460 nm) and S (1460–1530 nm) bands and even extends into C (1530–1565 nm) and L (1565–1625 nm) bands, implying that these glasses might be very useful for the applications in the high power or broadly tunable laser sources and the wide-band optical amplifiers.

Acknowledgments

The authors would like to acknowledge the financial supports provided by the National Natural Science Foundation of China (Grant No. 50125258 and 60377040), Shanghai Nanotechnology Promotion Center (Grant No. 0352nm042) and the State Key Lab for Advanced Photonic Materials and Devices, Fudan University.

References

[1] G. Keiser, Optical Fiber Communications, 3rd Ed., McGraw-Hill, New York, 2000, p. 10.
[2] M. Yamjada, H. Ono, Y. Ohishi, Electron. Lett. 34 (15) (1998) 1490.
[3] S. Tanabe, Glastechn. Ber. Glass Sci. Technol. C 74 (2001) 67.
[4] E.V. Zharikov, V.A. Smirnov, in: S.R. Rotman (Ed.), Wide-Gap Luminescent Materials: Theory and Applications, Kluwer Academic, Dordrecht, 1997, p. 13.
[5] S. Tanabe, X. Feng, Appl. Phys. Lett. 77 (6) (2000) 818.
[6] T. Suzuki, Y. Ohishi, Appl. Phys. Lett. 84 (19) (2004) 3804.
[7] Y. Fujimoto, M. Nakatsuka, Jpn. J. App. Phys. 40 (2001) L279.
[8] Y. Fujimoto, M. Nakatsuka, App. Phys. Lett. 82 (19) (2003) 3325.
[9] M. Peng, J. Qiu, D. Chen, X. Meng, L. Yang, X. Jiang, C. Zhu, Opt. Lett. 29 (17) (2004) 1998.
[10] L. Neindre, S. Jiang, B. Hwang, T. Luo, J. Watson, N. Peyghambarian, J. Non-Cryst. Solids 255 (1999) 97.
[11] K. Murata, Y. Fujimoto, T. Kanabe, H. Fujita, M. Nakatsuka, Fusion Eng. Des. 44 (1999) 437.
[12] S. Sen, J. Stebbins, J. Non-Cryst. Solids 188 (1995) 54.
[13] T. Fujiyama, T. Yokoyama, M. Hori, M. Sasaki, J. Non-Cryst. Solids 135 (1991) 198.
[14] I. Thomas, S. Payne, G. Wilke, J. Non-Cryst. Solids 151 (1992) 183.
[15] K. Arai, H. Namikawa, K. Kumata, T. Honda, Y. Ishii, T. Handa, J. App. Phys. 59 (10) (1986) 3430.
[16] S. Risbud, R. Kirkpatrick, A. Taglialavore, B. Montez, J. Am. Ceram. Soc. 70 (1) (1987) C-10.
[17] M. Shimbo, S. Tai, K. Tanzawa, J. Am. Ceram. Soc. 69 (1) (1986) 23.
[18] R.D. Shannon, Acta Cryst. A 32 (1976) 751.
[19] G. Blasse, A. Brill, J. Chem. Phys. 48 (1) (1968) 217.
[20] R. Reisfeld, L. Boehm, J. Non-Cryst. Solids 16 (1974) 83.
[21] J.A. Duffy, M.D. Ingram, Phys. Chem. Glasses 15 (1) (1974) 34.
[22] S. Parke, R.S. Webb, J. Phys. Chem. Solids 34 (1973) 85.
[23] G. Blasse, A. Meijerink, M. Nomes, J. Zuidema, J. Phys. Chem. Solids 55 (2) (1994) 171.
[24] A.M. Srivastava, J. Lumin. 78 (1998) 239.
[25] R. Retoux, F. Studer, C. Michel, B. Raveau, A. Fontaine, E. Dartyge, Phys. Rev. B 41 (1) (1990) 193.
[26] S. Salem-Sugui Jr., E.E. Alp, S.M. Mini, M. Ramanathan, J.C. Campuzano, G. Jennings, M. Faiz, Phys. Rev. B 43 (7) (1991) 5511.
[27] M.B. Volf, Glass Science and Technology, vol. 7, Elsevier, Amsterdam, 1984, p. 465.
[28] W. Dong, C. Zhu, J. Phys. Chem. Solids 64 (2003) 265.
[29] J. Yang, S. Dai, Y. Zhou, L. Wen, L. Hu, Z. Jiang, J. Appl. Phys. 93 (2) (2003) 977.